

## ENC-2022-0036

# RECORD HEAT FLUX FOR FLOW BOILING OF R123 IN A SINGLE MICROCHANNEL

Thalles Coimbra Borba Roldão

Juliana Silva Brasil

Cristiano Bigonha Tibiriçá

University of São Paulo, EESC, Heat Transfer Research Group; São Carlos, SP, Brazil, 13566-590.

[thallescbr@usp.br](mailto:thallescbr@usp.br)

[juliana.brasil@usp.br](mailto:juliana.brasil@usp.br)

[bigonha@sc.usp.br](mailto:bigonha@sc.usp.br)

**Abstract.** *This paper presents new data for flow boiling in microchannels with R123 as the working fluid. A single horizontal tube with an internal diameter of 1.1mm and heated length of 100mm was used. The experiments were conducted with values of mass velocity between 2000 and 4000 kg/m<sup>2</sup>s, a range above the data seen in the literature for this fluid, and high heat fluxes, ranging from 394 to 659 kW/m<sup>2</sup>, which is a record value for flow boiling with R123 in a single microchannel. The obtained heat transfer coefficients were up to 31 kW/m<sup>2</sup>K, which is also a record value for flow boiling of R123 in a single microchannel. Predictive methods to estimate the heat transfer coefficient were tested and mean absolute errors of 11.39% and 19.11% were obtained.*

**Keywords:** *Flow boiling, microchannel, R123.*

## 1. INTRODUCTION

There is a growing demand for dissipating high levels of heat on small surface area devices. Convective boiling has proved to be a very efficient way to exchange heat, once it takes advantage of sensible and latent heat of the working fluid, which represents an advantage over the use of single-phase heat exchangers. As pointed out by Lee e Mudawar (2009), the advantages of convective boiling are promoting a transition from the use of single-phase to two-phase heat exchanging in electrical devices. Furthermore, the application of microchannels has attracted attention in the last two decades due to its ability to deliver high heat fluxes with a compact structure (Tibiriçá et al, 2017). The halogenated refrigerant fluids are widely used in convective boiling experiments, but only a few works using R123 are reported in the literature. This fluid has an advantage over more used fluids, such as R134a, which is its low saturation pressure for the same temperature. One of the challenges in the use of microchannels, and one of the main limitations for the continue reduction of the size of compact heat exchangers is the high pressure drop that can occur during the flow boiling, as pointed out by Tibiriçá et al (2017), therefore the application of low pressure fluids, as R123, may be an option to operate systems that deliver high heat dissipation applying low pressures.

A literature review on R123 flow boiling works was made and the details of the experimental procedures and results are shown in Table 1. As can be seen in the table, and to the best of the authors's knowledge, there are no works in the literature with R123 with mass velocities above 3000 kg/m<sup>2</sup>s. The range of mass velocity found in the literature was between 55 and 2600 kg/m<sup>2</sup>s. Kosar and Peles (2007a) were able to attain high heat fluxes as close to 1MW/m<sup>2</sup> (considering the entire heat exchange area) with a heat sink with 5 microchannels, but the highest value of heat flux found on experiments conducted with single microchannels was only 0.43 MW/m<sup>2</sup> by Roday e Jansen(2009). Therefore, it is noticeable that more studies with R123 are needed operating with higher mass velocities and higher heat fluxes so that the fluid performance in these cases can be analyzed.

Taking this context into account, this paper presents very new experimental data on convective boiling with R123 in a single microchannel of 1.1mm internal diameter. The main objective here is to achieve high values of heat

flux and heat transfer coefficient with values of mass velocities above the used in the actual literature, in order to expand the data of flow boiling of R123 in a single microchannel.

Table 1. Literature review on R123 flow boiling experiments.

Author	Geometry / Number of tubes	Di (mm)	Lh (mm)	G (kg/m <sup>2</sup> s)	h <sub>max</sub> local (W/m <sup>2</sup> k)	q <sub>máx</sub> (MW/m <sup>2</sup> )
Singh et al (1995)	Circular/1	9,4mm	1220	400	30000	0,02
Bao et al (2000)	Circular/1	1.95	270	1800	~14000	0,2
Shneider, Kosar and Peles (2007)	Rectangular/5	0.227	10	1368	~14000	0,59 <sup>(2)</sup>
Kosar and Peles (2007a)	Rectangular/5	0,23 <sup>(1)</sup>	10	1118	Not informed	1,078 <sup>(2)</sup>
Kosar and Peles (2007b)	Rectangular/20	0.43 <sup>(1)</sup>	10	2349	~70000	0.75 <sup>(2)</sup>
Kuan e Kandlikar (2007)	Rectangular/6	0.546 <sup>(1)</sup>	63.5	533.8		0.201 <sup>(2)</sup>
Roday e Jansen (2009)	Circular/1	0.286	17.26	825	Not informed	0.43
In e Jeong (2009)	Circular/1	0.19	31	470	~8000	0,02
Kosar, Ozdemir e Keskinöz (2010)	Rectangular/20	0.43 <sup>(1)</sup>	10	1351	Not informed	0,67 <sup>(2)</sup>
Mikielewicz et al (2013)	Circular/1	1.15 – 2.3	385	900	Not informed	0.15
Seo e Bang (2015)	Circular/1	5.45	280	2600	Not informed	0.275
Hardik, Kumar e Prabhu (2017)	Circular/1	5.5 - 12	500-1000	1650	~10000	0.337
Hardik e Prabhu (2018)	Helicoidal/1	5.5 - 9.5	482	1501	~8000	0.344
Gorgy e Eckels (2019)	Circular/20	3.2	1000	55	~25000	0,06
Tank et al (2021)	Circular/1	11.9	400, 600, 1000	1210	~5500	0,151

(1) Hydraulic diameter

(2) Estimated to a single-channel

## 2. EXPERIMENTAL APPARATUS AND PROCEDURE

The experimental apparatus consists of refrigerant and water circuits. In the refrigerant circuit (Fig. 1), starting from the condenser, the fluid flows through a filter to the pump. A Coriolis mass flow meter is positioned between the filter and the pump. The desired mass flow rate is set up by a frequency controller acting on the pump and by a bypass piping line containing a needle valve that is installed between the inlet and the outlet of the pump. The bypass also ensures the system's security. A subcooler is installed after the condenser to ensure that the fluid entering the pump is subcooled. Downstream of the pump the fluid is directed to the test section, which is made of an unique 1.1mm internal diameter horizontal stainless-steel tube with 100mm of heated length. In the test section a DC power source is used to apply a current directly on the external surface of the tube to promote the boiling of the flowing fluid. Just upstream the sect section, the enthalpy of the liquid is estimated from its temperature by a thermocouple located at an adiabatic position on the outside tube wall, and its pressure by an absolute pressure transducer. Six thermocouples are installed across the tube in different diabatic positions to measure the temperature of the wall. Just downstream the test section another thermocouple located at an adiabatic position measures the outlet fluid temperature, which is taken as the reference saturation temperature, and the outlet pressure is estimated by another absolute pressure transducer. The location of the thermocouples on the test section can be seen in Figure 2. Downstream the test section the fluid is directed back to the condenser, formed by a tube-in-tube heat exchanger. A reservoir is positioned between the condenser and the pump to control the system's pressure. The pressure of the reservoir is controlled by its temperature once it is heated to a desired saturation temperature so that a desired saturation pressure is attained. Insulation materials are used across the whole piping to prevent heat exchange with the environment. The water circuit is used to pump cold water to the condenser and to the subcooler.

The experiments were conducted first by setting the temperature in the refrigerant tank. Once the temperature was set and the pressure of the system was stable, the mass velocity was set through the frequency controller acting on the pump. Heat flux was then applied to the test section to initiate evaporation. First the convective boiling was initiated with low mass velocities and low heat fluxes to avoid failure of the test section due to wall temperature oscillations. Once the boiling was initiated in the test section, the heat flux was progressively increased by incrementing the electrical current in small steps, letting the temperatures and pressures stabilize. This is also useful to avoid sudden rise

of the temperature of the tube. This procedure was repeated at each mass velocity tested. A data acquisition system was used to collect all the data and send it to a computer program that was used to control the system and save the data acquired.

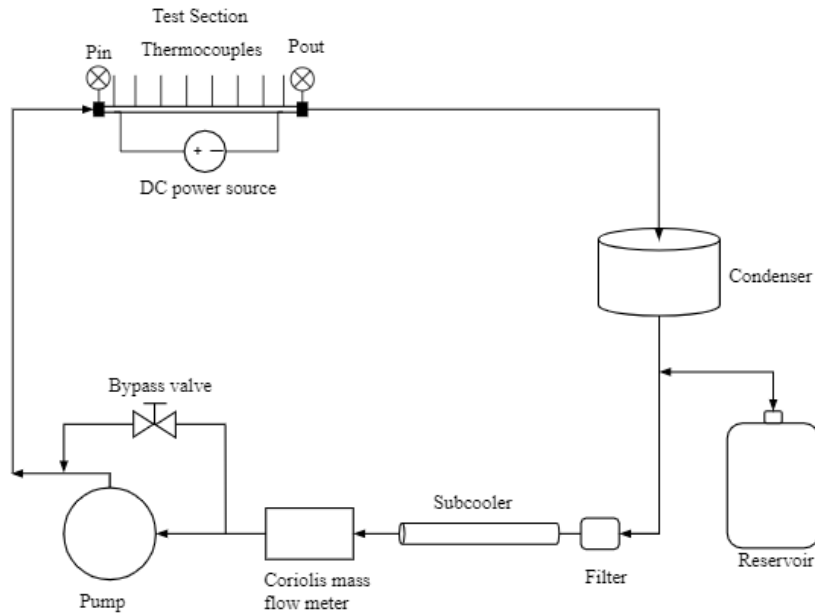


Figure 1. Refrigerant Circuit in the Experimental Apparatus

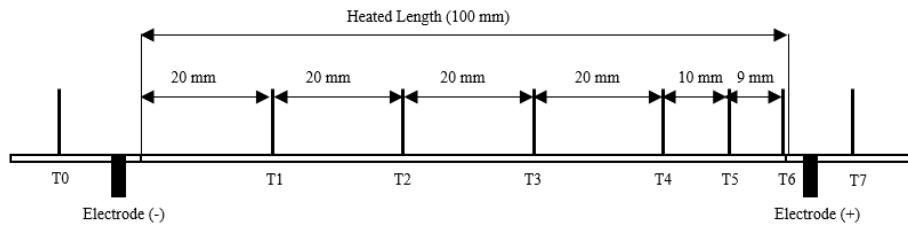


Figure 2. Test section with thermocouples positions.

### 3. DATA REDUCTION

In the present study the parameters of interest analyzed are the heat flux, the mass velocity, exit saturation temperature, local vapor quality, local heat transfer coefficient (HTC) and the pressure drop. The data reduction made here is similar to one performed in the work of Maestri (2021). The heat flux ( $q$ ) is obtained by the ratio between the electrical power ( $P$ ) supplied to the test section and its internal surface area ( $A$ ) based on the heated length ( $L_h$ ) and inside diameter ( $d_i$ ). The power supplied is given by the product between the electrical current ( $j$ ) and the voltage ( $V$ ) supplied by the DC power source, as in Equation (1). Mass velocity ( $G$ ) is given by the ratio between the mass flow rate ( $m$ ) given by the Coriolis flow meter and the internal cross-sectional area of the tube. The local heat transfer coefficient is calculated by the Newton's Cooling Law as in Equation (2), where  $T_w$  is the surface temperature of the inner tube wall, estimated by Fourier's Law based on temperature of the external surface of the wall and assuming one dimensional conduction, uniform heat generation in the tube and adiabatic external surface, all the heat being directed to the test fluid.  $T_{sat}(z)$  is the local saturation temperature of the fluid in a specified ( $z$ ) position. The local saturation temperature is estimated based on the pressure at the exit of the test section and the pressure drop along it.

$$q = \frac{P}{A} = \frac{V * j}{\pi d_i L_h} \quad (1)$$

$$h_{local} = \frac{q}{T_w - T_{sat}(z)} \quad (2)$$

The local heat transfer coefficient calculated with Equation (2) was compared with correlations for the HTC. The correlation of Gnielinski (1975) was used to compare the single-phase HTC used in the data validation, and the correlations of Liu and Winterton (1991) and Tibiriçá et al (2017) were used to compare with the two-phase HTC data obtained. The local vapor quality is obtained by an energy balance equation made over the test section, as seen in Equation (3), where  $i_{ms}$  is the enthalpy of the liquid at the inlet of the pre-heater and was estimated based on the measured temperature and pressure at the inlet;  $i_l(z)$  is the liquid enthalpy and  $i_{lv}(z)$  the latent heat of vaporization at the position  $z$ , and they were both estimated based on the fluid temperature measured at position ( $z$ ) and assuming a saturated state.

$$x(z) = \frac{(q\pi Dz/\dot{m}) + i_{ms} - i_l(z)}{i_{lv}} \quad (3)$$

During data validation, with single-phase flow, in order to validate the accuracy of the measured values, the pressure drop ( $\Delta P$ ) measured by the pressure transducers was compared with the theoretical value of pressure drop for single-phase flow in pipes obtained from Equation (4), where  $L$  is the length of the tube,  $f$  is the frictional coefficient, calculated with the correlation of Pethukov (1970),  $v$  is the velocity of the flow and  $\rho$  is the density of the fluid.

$$\Delta P = \frac{f \cdot L \cdot \rho \cdot v^2}{2 \cdot d_i} \quad (4)$$

#### 4. EXPERIMENTAL VALIDATION AND UNCERTAINTIES

Single-phase flow experiments were performed to assure the accuracy of the measured pressure drop, energy balance and heat transfer coefficient. The range of experimental parameters used during monophasic validation was a Reynolds Number range from 17400 to 29100, and heat fluxes from 59 to 145 kW/m<sup>2</sup>, with exit temperatures between 20 and 31°C.

During the experiments, it was assumed that all the energy provided to the test section would be absorbed by the working fluid. To validate this assumption, an energy balance was made with the single-phase experiments and compared to the power supplied to the test section, calculated with Equation (1). The Equation (5) was used to calculate the error associated with the heat transferred to the fluid, where  $P$  is the total power supplied,  $i_{out}$  is the enthalpy of the liquid at the outlet of the test section and  $i_{in}$  the enthalpy at the inlet. Figure 3 shows the results for the error associated with the energy balance over the test section during the single-phase tests. According to these tests, the inaccuracy of the heat flux calculation was less than around 5%, as shown in Figure 3.

To validate the pressure drop obtained with the pressure transducers, the measured pressure drop was compared with Equation (4), as mentioned in Section 3. Figure 4 shows the pressure drop results for the single-phase validation tests. The results were inside an error band of less than 10%.

$$E(\%) = \frac{(\pi d_i^2/4)G(i_{out} - i_{in}) - P}{P} * 100 \quad (5)$$

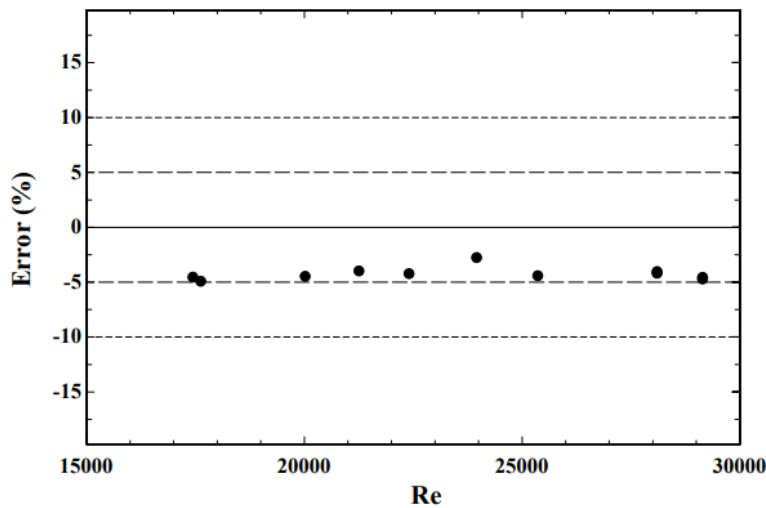


Figure 3. Energy Balance Validation.

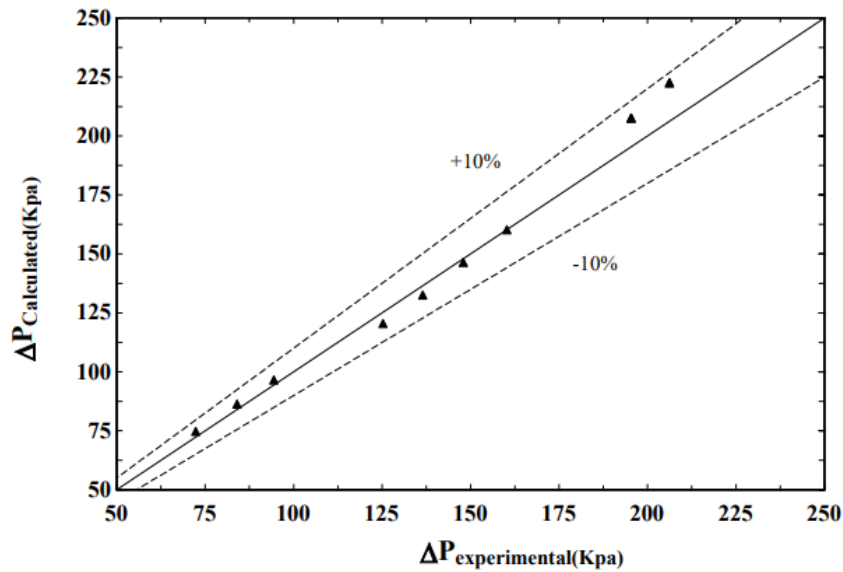


Figure 4. Pressure Drop Validation.

The experimental HTC calculated with Equation (2), and neglecting heat losses to the environment, was compared with the Gnielinski (1975) correlation for the single-phase experiments, as mentioned in section 3, in order to validate the measuring procedure of the heat transfer coefficient. The HTC is calculated to each point where a thermocouple is positioned. Within the heated length of the tube there are six thermocouples. The HTC calculated to four of these six points were compared with the theoretical values obtained with the correlation of Gnielinski (1975) and the results are shown in Figure 5, where h<sub>2</sub>, h<sub>3</sub>, h<sub>4</sub> and h<sub>5</sub> are related to the points shown in Figure 2. The results showed good agreement with the theory, all the points fitted in an error band of 30%.

Uncertainties for parameters involved in the experiment were estimated using the method of sequential perturbation, according to Moffat (1988), as mentioned by Maestri (2021). All thermocouples were calibrated and the temperature uncertainty was evaluated according to the procedure suggested by Abernethy and Thompson (1973). The experimental uncertainties are listed in Table 2, depicting the uncertainties of the measured and calculated parameters and including the maximum uncertainties of the vapor quality and heat transfer coefficient. The uncertainty of the HTC is related to the results shown in Figure 5, and the uncertainty of the vapor quality is related to the heat uncertainty shown in Figure 3.

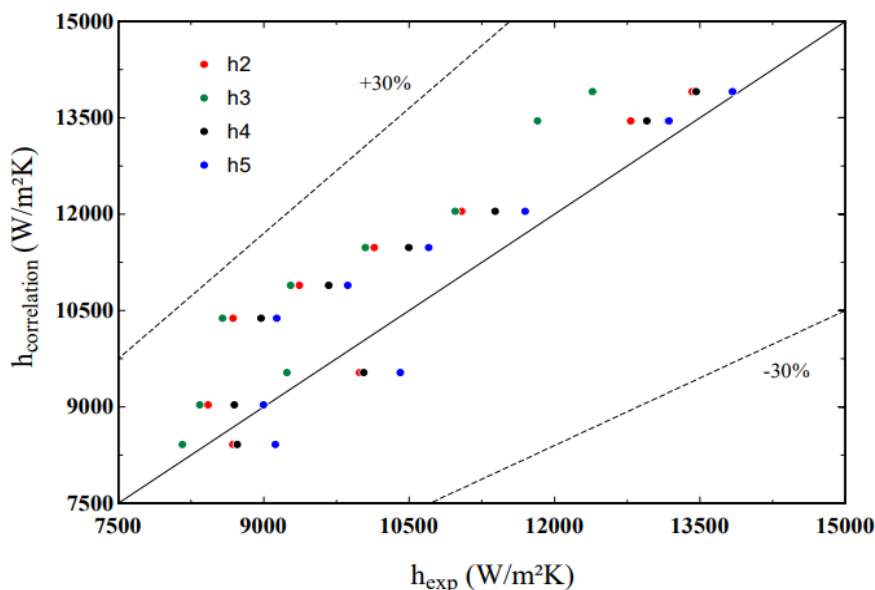


Figure 5. HTC validation.

Table 2. Uncertainty of measured and calculated parameters.

Parameter	Uncertainty	Parameter	Uncertainty
D	20 $\mu\text{m}$	x	<5%
L	0.2 mm	P <sub>measured</sub> / P <sub>calculated</sub>	1 kpa / < 10%
G	0.8 %	T	0.5°C
q	< 5%	h	<25%

## 5. EXPERIMENTAL RESULTS

In this section the two-phase experimental points obtained in this paper are described. Figure 6 shows the local HTC results for point 5 (see Figure 2) in the test section, where two-phase flow was already established, with increasing heat flux for five different values of mass velocity: 2000, 2500, 3000, 3500 and 4000 kg/m<sup>2</sup>s. Heat fluxes between 394 and 659 Kw/m<sup>2</sup> were achieved. It is clear that the HTC increases with the increase of heat flux for all the values of mass velocity, as expected. The inlet temperature and the saturation temperature were not kept constant, so the values of the HTC for the different mass velocities should not be compared in the figure.

The figure shows that the experimental facility was able to achieve high values of HTC during flow boiling of R123 with values around 31 kW/m<sup>2</sup>K, which is a record value for flow boiling of R123 in a single microchannel, as can be seen in Table 1. The highest values of heat flux obtained in this research are also records heat flux for flow boiling of R123 in a single microchannel, since the highest value found in the literature for these conditions was around 430 kW/m<sup>2</sup>K, to the best of the author's knowledge, as shown in Table 1. The range of mass velocity used was also highest than the range found in the literature, as seen in Table 1.

The results were also used to evaluate the accuracy of the correlation to predict the HTC of Liu and Winterton (1991) and Tibiriçá et al (2017). Figure 7 shows the comparison of the experimental results for the local HTC at the same point used in Figure 6, the point 5 in the test section (see Figure 2), with the values predicted by the correlations of Tibiriçá et al (2017) and Liu and Winterton (1991). The figure shows that both correlations were able to predict the results for the local HTC relatively well. The correlation of Tibiriçá et al (2017) presented the best predictive results with a mean absolute error (MAE) of 11.39%. Liu and Winterton (1991) had a MAE of 19.11%.

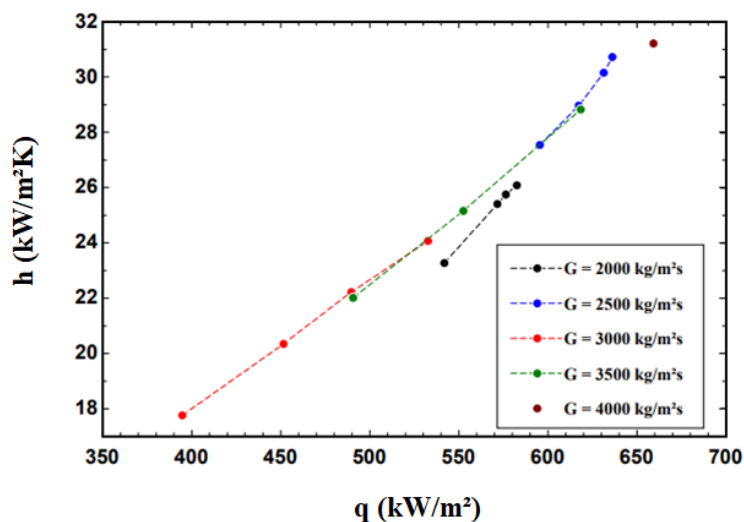


Figure 6. Experimental data points.

## 6. CONCLUSIONS

This paper has presented new experimental results for flow boiling in a 1.1mm internal diameter microchannel with R123 as the working fluid, operating with high mass velocities, heat fluxes and heat transfer coefficients compared with the data found in the literature. The experiments were performed with mass velocities of 2000, 2500, 3000, 3500 and 4000 kg/m<sup>2</sup>s. The higher value of mass velocity found in the literature was 2600 kg/m<sup>2</sup>s. Heat fluxes ranging from 394 to 659 kW/m<sup>2</sup> and heat transfer coefficients between 15 to 31 kW/m<sup>2</sup>K were achieved. The heat flux and the heat transfer coefficient obtained in this paper are record values for flow boiling of R123 in a single microchannel, to the best of the author's knowledge. The HTC results were compared with the predictive methods of Tibiriçá et al (2017) and Liu and Winterton (1992). Both provided relatively good agreement with the experimental data with mean absolute

errors of 11.39% and 19.11% respectively. The results shows that the experimental apparatus is able to perform experiments of flow boiling in microchannels with R123 with high mass velocities, heat fluxes and heat transfer coefficients and new experimental data shall be collected in future experiments including studies of critical heat flux of R123 in microchannels.

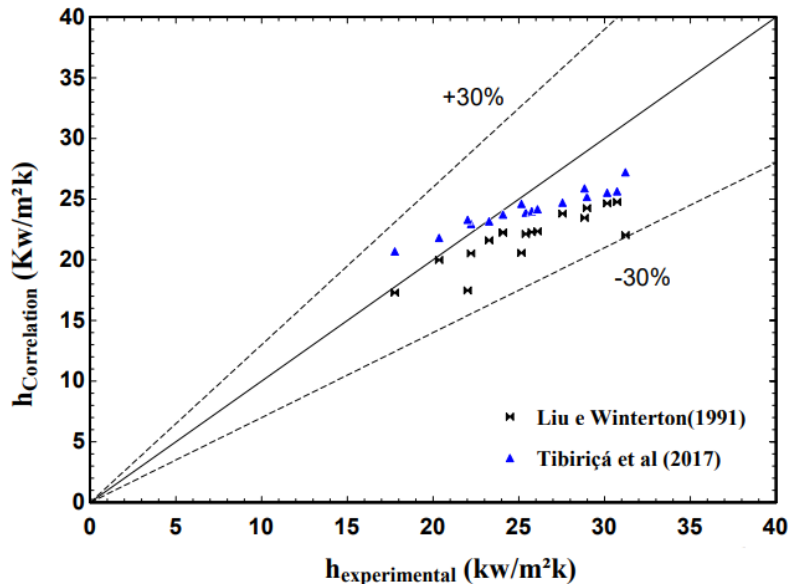


Figure 7. Comparison of experimental HTC with predicted values

## 7. ACKNOWLEDGEMENTS

The authors acknowledge FAPESP (grant 2019/11066-9 and 2021/10323-8, São Paulo Research Foundation), CAPES (Coordination for the Improvement of Higher Education Personnel, Finance Code 001) and CNPq (National Council for Scientific and Technological Development, process 304972/2017-7) for funding researches that have contributed to this study.

## 8. REFERENCES

- Abernethy, R. B., and Thompson, J. W.; (1973). Handbook Uncertainty in Gas Turbine Measurements, Arnold Engineering Development Center, Arnold Air Force Station, TN.
- Bao, Z.; Fletcher, D.; Haynes, B.; (2000). Flow boiling heat transfer of freon R11 and HCFC123 in narrow passages, *Int. J. Heat Mass Transfer* 43, 3347-3358.
- Gorgy, E.; Eckels, S.; (2019). Convective boiling of R-123 on enhanced-tube bundles. *International Journal of Heat and Mass Transfer*, 134, 752-767.
- Gnielinski, Volker.; (1975). New equations for heat and mass transfer in the turbulent flow in pipes and channels. *STIA*, v. 41, n. 1, p. 8-16.
- Hardik, B.; Kumar, G.; Prabhu, S.; (2017). Boiling pressure drop, local heat transfer distribution and critical heat flux in horizontal straight tubes. *International Journal of Heat and Mass Transfer*, Elsevier, v. 113, p. 466–481.
- Hardik, B.; Prabhu, S.; (2018). Boiling Pressure Drop, Local Heat Transfer Distribution And Critical Heat Flux In Helical Coils With R123. *International Journal of Thermal Sciences*, Elsevier v. 125, p. 149–165.
- In, S.; Jeong, S.; (2009). Flow boiling heat transfer characteristics of R123 and R134a in a micro-channel. *International Journal of Multiphase Flow* 35, 987–1000.

- Kosar, A.; Özdemir, M.; Keskinöz, M.; (2010). Pressure drop across micro-pin heat sinks under unstable boiling conditions. *International Journal of Thermal Sciences* 49,1253 - 1263.
- Kosar, A.; Peles, Y.; (2007a). Critical heat flux of R-123 in silicon-based microchannels, *J. Heat Transf.* 129 (7), 844–851.
- Kosar, A.; Peles, Y.; (2007b). Boiling heat transfer in a hydrofoil-based micro pin fin heat sink. *International Journal of Heat and Mass Transfer*, Elsevier, v. 50, n. 5-6, p. 1018–1034.
- Kuan, W.; Kandlikar, S.; (2007). Critical heat flux measurement and model for refrigerant-123 under stabilized flow conditions in microchannels. In: *AMERICAN SOCIETY OF MECHANICAL ENGINEERS DIGITAL COLLECTION*. ASME International.
- Lee, J. Mudawar, I.; (2009). Critical heat flux for subcooled flow boiling in micro-channel heat sinks. *International Journal of Heat and Mass Transfer*, v.52, p. 3341-3352,
- Liu, Z.; Winterton, R.; (1991). A general correlation for saturated and subcooled flow boiling in tubes and annuli, based on a nucleate pool boiling equation. *Int J Heat Mass Transf* 34:2759–2766.
- Maestri, R. Study of the critical heat flux and film boiling at high velocities and temperatures. Dissertation (Master 's Degree) - Universidade de São Paulo, 2021.
- Mikielewicz, D.; Wajs, J.; Glinski, M.; Zrooga, A.; (2013). Experimental investigation of dryout of ses 36, r134a, r123 and ethanol in vertical small diameter tubes. *Experimental thermal and fluid science*, Elsevier, v. 44, p. 556–564, 2013.
- Moffat, R. J.; (1988). Describing the Uncertainties in Experimental Results. *Exp. Thermal Fluid Sci.*, 1, pp. 3–17.
- Pethukov, B. S., in T.F. Irvine and J. P. Hartnett, Eds., *Advances in Heat Transfer*, Vol. 6, Academic Press, New York, 1970.
- Roday, A.; Jensen, M.; (2009). Study of the critical heat flux condition with water and r-123 during flow boiling in microtubes. part i: Experimental results and discussion of parametric effects. *International Journal of Heat and Mass Transfer*, Elsevier, v. 52, n. 13-14, p.3235–3249.
- Seo, B.; Bang, I.; (2015). Effects of al2o3 nanoparticles deposition on critical heat flux of r-123 in flow boiling heat transfer. *Nuclear Engineering and Technology*, Elsevier, v. 47, n. 4, p.398–406.
- Singh, M.; Serguei, O.; Dessiatoun, W.; (1995). Chu. In-Tube Boiling Heat Transfer Coefficients of R-123 and their Enhancement Using the EHD Technique. *Journal of Enhanced Heat Transfer*, v2, , p 209-217.
- Schneider, B.; Kosar, A.; Peles, Y.; (2007). Hydrodynamic cavitation and boiling in refrigerant (R-123) flow inside microchannels. *International Journal of Heat and Mass Transfer* 50, 2838–2854.
- Tank, P.; Hardik, B.; Sridharan, A.; Prabhu, S.; (2021). Pressure drop, local heat transfer coefficient, and critical heat flux of DNB type for flow boiling in a horizontal straight tube with R-123. *Heat and Mass Transfer*, 57, 223–250.
- Tibiriçá, C. B.; Rocha, D. M. ; Sueth Jr., I. L. S. ; Bochio, G.; Shimizu, G. K. K. ; Barbosa, M. C. ; Ferreira, S. S. (2017). A complete set of simple and optimized correlations for microchannel flow boiling and two- phase flow applications. *Applied Thermal Engineering*, v. 126, p. 774-795

## 9. RESPONSIBILITY NOTICE

The authors are the only responsible for the printed material included in this paper.